



## Identification of novel SAR properties of the Jak2 small molecule inhibitor G6: Significance of the *para*-hydroxyl orientation

Rebekah Baskin<sup>a</sup>, Meghanath Gali<sup>b</sup>, Sung O. Park<sup>a</sup>, Zhizhuang Joe Zhao<sup>c</sup>, György M. Keserű<sup>d</sup>, Kirpal S. Bisht<sup>b</sup>, Peter P. Sayeski<sup>a,\*</sup>

<sup>a</sup> Department of Physiology and Functional Genomics, University of Florida, Gainesville, FL, USA

<sup>b</sup> Department of Chemistry, University of Florida, South Florida, Tampa, FL, USA

<sup>c</sup> Department of Pathology, University of Oklahoma Health Sciences Center, Oklahoma City, OK, USA

<sup>d</sup> Department of General and Analytical Chemistry, Budapest University of Technology and Economics Budapest, Hungary

### ARTICLE INFO

#### Article history:

Received 6 October 2011

Revised 5 December 2011

Accepted 8 December 2011

Available online 21 December 2011

#### Keywords:

Jak2 tyrosine kinase

G6

Small molecule inhibitor

Stilbenoid

SAR

### ABSTRACT

In this study, we analyzed the structure–activity relationship properties of the small molecule Jak2 inhibitor G6. We synthesized a set of derivatives containing the native *para*-hydroxyl structure or an alternative *meta*-hydroxyl structure and examined their Jak2 inhibitory properties. We found that the *para*-hydroxyl derivative known as NB15 had excellent Jak2 inhibitory properties in silico, in vitro, and ex vivo when compared with *meta*-hydroxyl derivatives. These results indicate that NB15 is a potent derivative of the Jak2 inhibitor G6, and that maintaining the *para*-hydroxyl orientation of G6 is critical for its Jak2 inhibitory potential.

© 2011 Elsevier Ltd. All rights reserved.

Janus kinase 2 (Jak2) is a member of the Janus family of non-receptor tyrosine kinases and plays a key role in numerous signaling pathways regulating cell survival, proliferation, and differentiation. Jak2 forms associations with growth factor and cytokine receptors, and upon activation, it phosphorylates substrates such as the Signal Transducers and Activators of Transcription (STATs).<sup>1–4</sup> Activated STAT proteins then translocate to the nucleus to modulate gene transcription. Mutations in Jak2 can lead to constitutive activation of the kinase and thus cause aberrant downstream Jak-STAT signaling. Specifically, the Jak2-V617F mutation occurs within the pseudo-kinase domain of Jak2 and relieves the auto-inhibitory function of this domain, thus allowing the kinase domain to be constitutively active in the absence of ligand.<sup>5,6</sup>

In 2005, the Jak2-V617F mutation was discovered in a large number of myeloproliferative neoplasm (MPN) patients.<sup>7–11</sup> These patients suffer from an overproduction of blood cells of the myeloid lineage. This heterogeneous group of diseases includes polycythemia vera (PV), essential thrombocythemia (ET) and primary myelofibrosis (PMF). The Jak2-V617F mutation occurs in over 90% of PV patients and a large subset of ET and PMF patients. This mutation has also been shown to cause MPN phenotypes in bone marrow transplant and transgenic mouse models.<sup>12,13</sup> Currently, there are no effective therapies for these diseases beyond palliative

treatments such as hydroxyurea and phlebotomy. Therefore, Jak2 has been investigated in recent years as a potential therapeutic target, and a number of compounds are in pre-clinical and clinical development.<sup>14</sup>

Our lab recently used an in silico drug discovery approach to develop a Jak2 small molecule inhibitor known as G6.<sup>15</sup> We have shown that G6 inhibits Jak2-mediated pathologic cell growth using in vitro cell culture models, in vivo models, and ex vivo patient samples.<sup>16</sup> We also demonstrated that the stilbene core structure of G6 is essential for its activity as a Jak2 inhibitor, in vitro and ex vivo.<sup>17</sup> Here, we further examined the structure of G6 to determine if structural modifications of the compound could enhance its Jak2 inhibitory potential. We hypothesized that the structure of G6 could be minimized in order to enhance its Jak2 inhibitory potential and that maintaining the *para*-hydroxyl orientation is required for Jak2 inhibition. To test this, we synthesized a set of G6 derivatives with different structural features and examined their in silico Jak2 binding properties and their effects on Jak2-mediated pathologic cell growth in vitro and ex vivo.

The structure of G6 consists of a stilbene core with ethyl groups attached to each carbon of the core, *para*-hydroxyl groups on each benzene ring, and tertiary amine moieties at the *meta* position of each ring (Supplementary data Fig. 1). In order to examine the structure–function correlations of this compound, we synthesized four structurally minimized G6 derivatives containing the native *para*-hydroxyl structure or an alternative *meta*-hydroxyl structure

\* Corresponding author.

E-mail address: [psayeski@ufl.edu](mailto:psayeski@ufl.edu) (P.P. Sayeski).

(Scheme 1, Supplementary data Fig. 1). These are known as NB4, NB6, NB13, and NB15. Compounds NB-4, -6, -13, and -15 were synthesized from stilbenoids 1–4 (Scheme 1). The chemical structures of the stilbenoids obtained were confirmed by  $^1\text{H}$  and  $^{13}\text{C}$  NMR analysis. Experimental details are provided in the Supplementary data.

The Jak2 ATP-binding pocket contains several critical regions involved in catalysis, including the hinge region, the glycine loop, the catalytic loop and the activation loop. The glycine loop is important for substrate and nucleotide binding. The hinge region contains Glu930 and Leu932, which interact with the adenine group of ATP. The activation loop contains the tyrosine 1007/1008 residues that, once phosphorylated, allow this region to undergo a conformational change to accommodate substrate binding. The catalytic loop contains residue Arg980 which is involved in the coordination of magnesium ions.<sup>18</sup> Each of the G6 derivatives was docked into the Jak2 ATP-binding pocket using AutoDock 4.2 (Scripps).<sup>19,20</sup> Fig. 1 shows the most favorable docking orientation for each compound. NB13 and NB15 showed interactions very similar to those of the parent compound, G6.<sup>17</sup> These include hydrogen bonds with residues in the hinge region, the activation loop, and the catalytic loop. NB4 and NB6 showed hydrogen bond interactions with several residues, but lacked any interactions with the critical hinge region residues, Glu930 or Leu932. These results indicate that the *para*-hydroxyl derivatives (NB13 and NB15) most closely mimic the in silico Jak2 binding properties of G6.

G6 is known to inhibit the proliferation of human erythroleukemia (HEL) cells in vitro and in vivo.<sup>16</sup> The HEL cell line is homozygous for the Jak2-V617F mutation and is highly proliferative due to constitutive Jak2 kinase activity. Therefore, we examined the ability of the four G6 derivatives to inhibit HEL cell growth. We found that NB15 had the most potent effect on HEL cell growth in both a dose- and time-dependent manner (Fig. 2A and B, respectively). This compound demonstrated 50% cell death at a concentration of  $\sim 0.85\ \mu\text{M}$  and completely blocked cell growth at all time points measured (Fig. 2B). The other derivatives had varying levels of cell growth inhibition, with NB6 consistently showing the lowest level of inhibition.

In order to determine the effects of these compounds on another Jak2-V617F-positive cell line, we examined their impact on cell growth in the Ba/F3-EpoR-Jak2-V617F cell line. This murine pro B cell line has been retrovirally transduced with the Jak2-V617F cDNA and demonstrates cytokine independent growth. We found that again NB15 was highly effective at inhibiting cell growth in both a dose- and time-dependent manner (Fig. 2C and D, respectively). Also, NB6 consistently had little impact on cell growth, except in this case at the highest concentration (Fig. 2C).

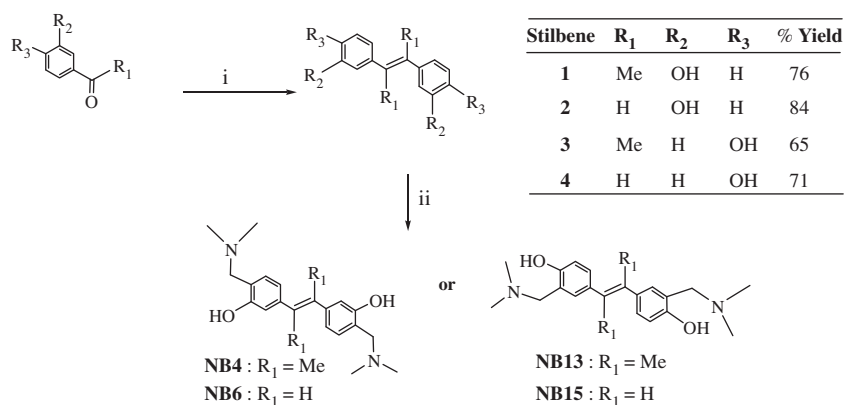
In order to determine if the reduced cell growth inhibitory potential observed in Fig. 2 correlated with reduced Jak2 kinase

activity, Jak2 in vitro kinase assays were carried out in the presence of a known Jak2 substrate, STAT1. Experimental details are presented in the Supplementary data. We found that NB15 significantly reduced Jak2 autophosphorylation (Table 1, Supplementary data Fig. 2). Both NB15 and NB13 significantly reduced the ability of Jak2 to phosphorylate the STAT1 substrate whereas the two *meta*-hydroxyl compounds had no significant effect on Jak2 autophosphorylation or STAT1 phosphorylation (Table 1, Supplementary data Fig. 2).

Jak2 directly activates the transcription factor STAT5 by phosphorylation at Tyr 694. STAT5 activation plays an important role in HEL cell proliferation, as STAT5 is known to regulate several pro-survival genes.<sup>21,22</sup> We have previously shown that G6 reduces STAT5 phosphorylation in HEL cells.<sup>17</sup> Therefore, we wanted to determine whether specific structural features in G6 correlate with reduced STAT5 phosphorylation in these cells. Fig. 3A shows a representative phospho-STAT5 blot and Fig. 3B shows the densitometric quantification of all experiments. We found that only the *para*-hydroxyl derivative NB15 was able to significantly reduce STAT5 phosphorylation when compared to vehicle treated control cells (Fig. 3).

Constitutively active Jak-STAT signaling leads to increased cell proliferation and inhibition of apoptosis. We have previously shown that the mechanism by which G6 decreases HEL cell viability is induction of cell cycle arrest and apoptosis.<sup>16</sup> Therefore, we wanted to determine if specific changes in compound structure correlate with changes in cell cycle properties and/or apoptosis. We found that NB15 and NB4 caused a significant increase in the number of cells in G2 with a corresponding decrease in G1, indicating a G2/M phase arrest (Fig. 4A). In order to further confirm the G2/M arrest, we examined the levels of several cell cycle regulatory proteins via Western blot analysis. We found that treatment with NB15 and NB4 caused a reduction in cyclin A expression, but had no effect on cyclin B1 or CDK1 expression (Fig. 4B). The other compounds had no effect on cyclin A, cyclin B or CDK1 expression (Fig. 4B). During cell cycle progression, CDK1 forms associations with both cyclin A and cyclin B1 in order to promote mitotic entry.<sup>23,24</sup> Therefore, it appears that NB15 and NB4 may cause G2 arrest due to decreased cyclin A expression and a subsequent block of mitotic entry.

We also wanted to examine the effects of each of the derivative compounds on apoptosis. We found that NB15, NB13, and NB4 induced apoptosis in HEL cells whereas NB6 was without effect (Fig. 4C). We further confirmed the induction of apoptosis by examining expression of apoptotic markers via Western blot. We examined cleavage of poly (ADP-ribose) polymerase, a hallmark of apoptosis. Additionally, we examined the cleavage of Bid, Bim



**Scheme 1.** Reagents and conditions: (i)  $\text{TiCl}_4$ , Zn, Dry, THF, reflux; (ii) Paraformaldehyde, dimethyl amine, MeOH, reflux.

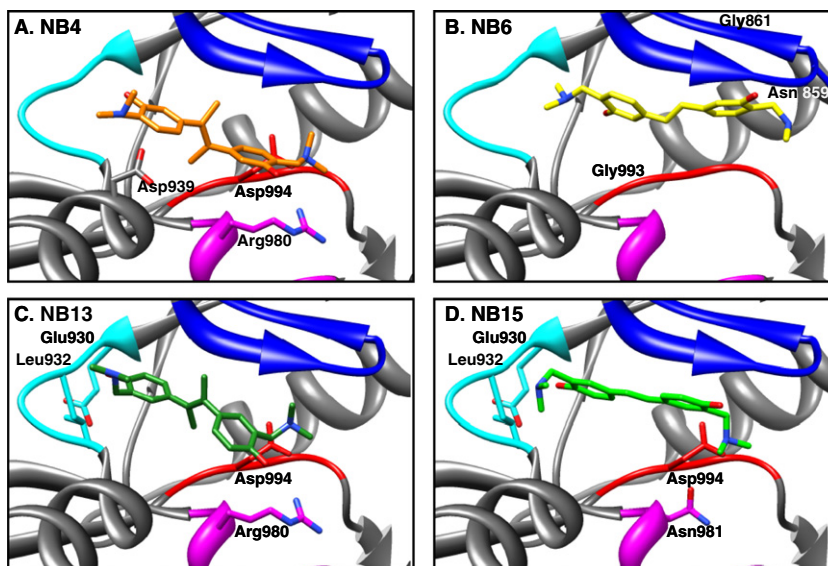


**Figure 1.** Molecular docking of the NB compounds. Each compound was computationally docked into the ATP-binding pocket of the Jak2 kinase domain (PDB code 3E64). The protein structure is represented as a ribbon, with the compounds shown as sticks. Colored regions of the protein are the glycine loop (blue), the hinge region (cyan), the catalytic loop (magenta) and the activation loop (red). Amino acid residues that participate in hydrogen bond interactions are shown as sticks and are labeled.

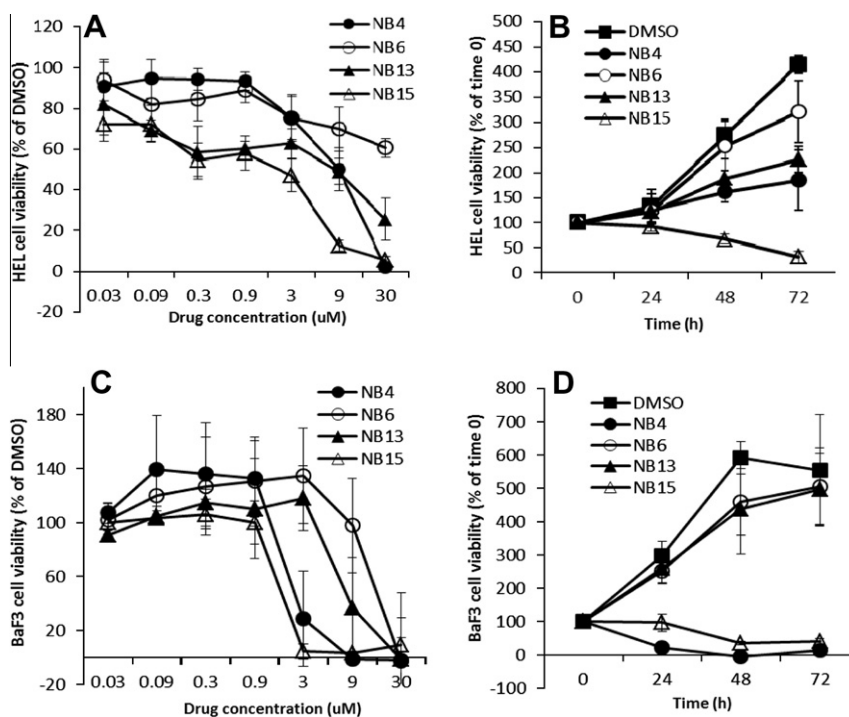


**Figure 2.** Effects of the G6 derivatives on HEL and Ba/F3-EpoR-Jak2-V617F cell proliferation. A, HEL cells were treated with the indicated concentrations of each compound for 72 h and cell viability was determined by trypan blue exclusion. B, HEL cells were treated with a 10  $\mu$ M concentration of each drug for the indicated periods of time and viability was determined by trypan blue exclusion. C, Ba/F3-EpoR-Jak2-V617F cells were treated with the indicated concentrations for 72 h and cell viability was determined by MTS assay. D, Ba/F3-EpoR-Jak2-V617F cells were treated with a 10  $\mu$ M concentration for the indicated times and viability was determined by MTS assay. Shown are results from two independent experiments, each performed in triplicate.

and caspase-3. Bid and Bim are pro-apoptotic factors that have been shown to be cleaved into active forms during apoptosis via the intrinsic pathway, and caspase-3 is an effector caspase that is also cleaved into its active form during apoptosis.<sup>25–27</sup> We found that NB15, NB13, and NB4 induced cleavage of PARP while NB6 did not (Fig. 4D). NB4 also caused cleavage of caspase-3 (Fig. 4D). However, only NB15 induced cleavage of PARP and caspase-3, along with cleavage of Bid and Bim (Fig. 4D).

It has been shown that Jak2-V617F transgenic mice develop a mixed MPN phenotype, with pathologically high numbers of erythrocytes, white cells and platelets.<sup>13</sup> We have shown that G6 has efficacy in this transgenic model, as it is able to normalize the cell counts and cause a reversal of other disease symptoms.<sup>28</sup> Therefore, we wanted to determine if specific structural changes to G6 correlate with the ability to reduce the clonogenic growth potential of bone marrow cells obtained from the Jak2-V617F transgenic

**Table 1**  
Inhibition of Jak2 in vitro kinase activity

	In vitro Jak2 phosphorylation (% of control)	In vitro STAT1 phosphorylation (% of control)
<b>NB4</b>	98.41 ± 2.69	103.85 ± 20.70
<b>NB6</b>	94.37 ± 30.16	93.31 ± 9.52
<b>NB13</b>	89.10 ± 13.13	89.14 ± 2.69*
<b>NB15</b>	44.24 ± 12.01*	71.48 ± 10.53*

\*  $p < 0.05$  versus DMSO control.

mice. For this, cells were isolated and cultured *ex vivo* in the presence of each compound for 0, 12, or 24 h, then transferred to methylcellulose media and cultured for an additional 6 days at which time the number of erythroid burst forming units (BFU-E) and granulocyte/macrophage colony forming units (CFU-GM) were counted. We found that NB4 significantly reduced the number of BFU-E and CFU-GM after 12 and 24 h of treatment (Fig. 5A). The only observed effect with NB6 was a significant reduction in the numbers of CFU-GM at the 24 hour time point (Fig. 5B). NB13 significantly reduced both the numbers of BFU-E and CFU-GM, but only after 24 h (Fig. 5C). Lastly, we found that NB15 significantly reduced or completely eliminated all clonogenic growth potential (Fig. 5D).

The results obtained here are interesting for a number of reasons. Firstly, our molecular docking results indicated that the two *para*-hydroxyl compounds, NB13 and NB15, interact with the Jak2 ATP-binding pocket through hydrogen bonds with the hinge region, the activation loop, and the catalytic loop. In contrast, the *meta*-hydroxyl compounds, NB4 and NB6, interacted with the activation and catalytic loops, but lacked an interaction with the hinge region. It has previously been shown that the hinge region is an important area to target for Jak2 inhibition as it interacts with the adenine group of ATP.<sup>18</sup> Our structure–function correlations determined here support the importance of the hinge region in

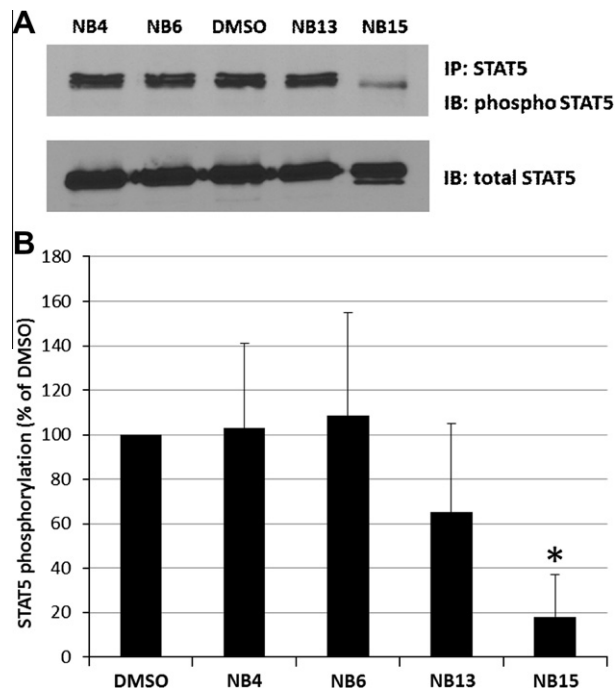


**Figure 3.** Effects of the G6 derivatives on STAT5 phosphorylation in HEL cells. A, HEL cells were treated with a 25  $\mu$ M concentration of each compound for 24 h and lysates were immunoprecipitated for STAT5 and Western blot was used to detect phospho-STAT5. Shown is one of four representative results. B, Quantification of STAT5 phosphorylation, measured as a percent of total and normalized to the DMSO control.  $n = 4$ . \*,  $p < 0.05$  versus DMSO.

Jak2 kinase inhibition as the two *meta*-hydroxyl compounds exhibited either moderate (NB4) or poor (NB6) Jak2 inhibitory potential *in vitro* when compared with NB13 and NB15.

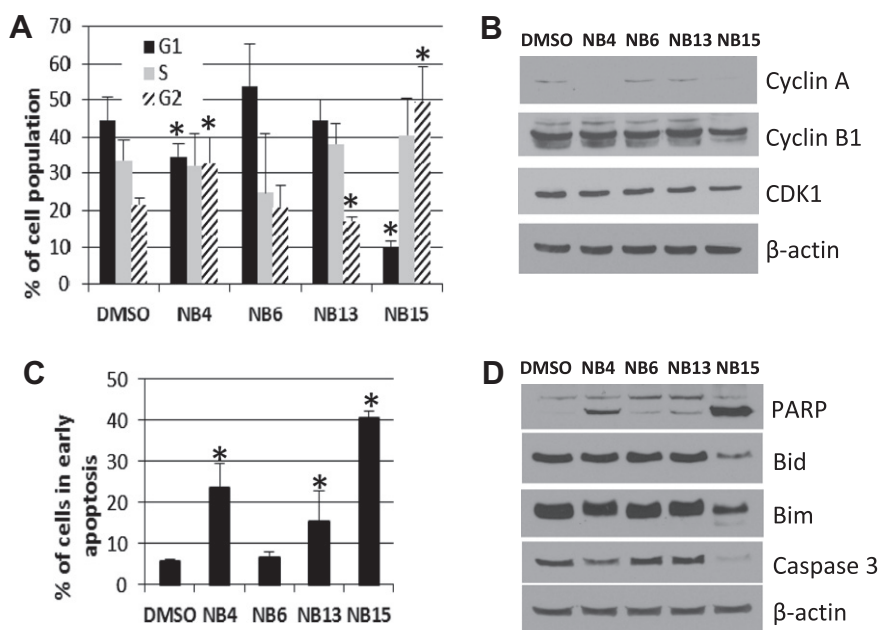


**Figure 4.** Induction of cell cycle arrest and apoptosis in HEL cells. A, Cells were treated with a 10  $\mu$ M concentration of each compound for 24 h and analyzed by flow cytometry for DNA content. Shown are results from two experiments, each measured in triplicate. \*,  $p < 0.05$ . B, Western blot was performed on cells treated with a 25  $\mu$ M concentration for 24 h to examine cyclin A, cyclin B1, and CDK 1 expression.  $\beta$ -actin was used as a loading control. Shown is one of two independent results. C, Cells were treated with a 10  $\mu$ M concentration of each compound for 48 h and analyzed by flow cytometry for Annexin V and propidium iodide staining. Plotted are the percentages of cells in early apoptosis (Annexin V positive, propidium iodide negative). Shown are the results from two independent experiments, each performed in triplicate. \*,  $p < 0.05$ . D, Western blot analysis was performed on cells treated with a 25  $\mu$ M concentration of each compound for 24 h to examine expression of PARP, Bid, Bim, and caspase 3. Shown is one of two representative results for each blot.

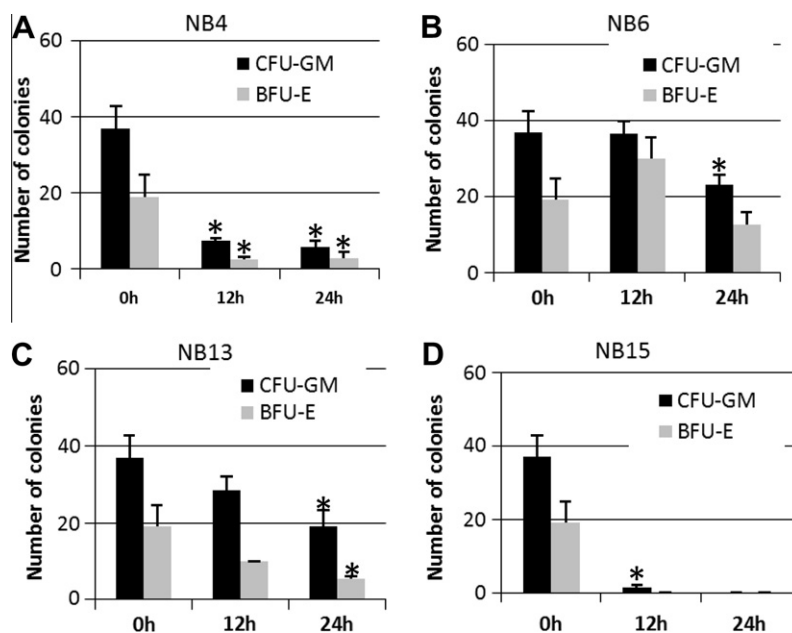


**Figure 5.** Effects of the G6 derivatives on the ex vivo clonogenic growth potential of Jak2-V617F-positive, murine bone marrow cells. Bone marrow cells were isolated from 6 month old Jak2-V617F transgenic mice and were incubated with media containing a 25  $\mu$ M concentration of each drug for 0, 12, or 24 h. Cells were then washed and plated in semi-solid media, and the number of BFU-E and CFU-GM were counted 6 days later. Panels A–D show the results for NB4, NB6, NB13, and NB15, respectively. Each condition was measured in duplicate. \*,  $p < 0.05$  versus 0 h.

It is also notable that, although NB13 and NB15 both demonstrated in silico Jak2 binding and in vitro Jak2 kinase inhibition, NB13 was still much weaker than NB15 as a Jak2 inhibitor as measured by the cell-based assays. Overall, these results indicate that the *para*-hydroxyl orientation on a stilbene scaffold alone is not sufficient to confer Jak2 inhibitory activity, but appears to be a necessary component.

Interestingly, NB4 was able to inhibit Jak2-mediated cell growth and induce apoptosis and cell cycle arrest. However, it was unable to reduce in vitro Jak2 kinase activity or reduce STAT5 phosphorylation in HEL cells. Furthermore, it demonstrated weak binding interactions with Jak2 in silico. Therefore, we believe the effects of NB4 on cell growth are via Jak2-independent mechanisms and underscore the importance of the *para*-hydroxyl structure in not only maintaining potency, but also specificity.

The results obtained with NB6 are also of interest. This *meta*-hydroxyl derivative had a minimized stilbene core. We found that it had the poorest Jak2 binding properties in silico and was largely without effect in the protein and cell based assays performed in vitro. From this, we conclude that minimization of the stilbene core on the *meta*-hydroxyl scaffold results in poor Jak2 inhibitory potential.

Stilbene compounds such as resveratrol and its derivatives have been implicated as potential therapeutic agents for hematological malignancies. These compounds have antioxidant properties, but also induce apoptosis and cell cycle arrest in leukemia cells.<sup>29</sup> It has been shown that the positioning of hydroxyl groups in resveratrol derivatives greatly impacts their antioxidant and cell growth inhibitory potential. Interestingly, the overall cytotoxic effects of *para*-hydroxyl resveratrol derivatives are lower than those of *ortho*-hydroxyl derivatives.<sup>29</sup> This may indicate that using a *para*-hydroxyl stilbene scaffold for the development of tyrosine kinase inhibitors may be beneficial in reducing non-specific cytotoxicity. Also, this type of structure allows for manipulation of other groups, such as amine moieties, in order to enhance the specificity for the target protein.

The parent compound, G6, has previously been shown to interact with Jak2 in silico via hydrogen bond interactions with the hinge region, the activation loop, and the catalytic loop.<sup>17</sup> Additionally, we have previously shown that G6 inhibits HEL cell proliferation and induces apoptosis and cell cycle arrest.<sup>16</sup> Of the four G6 derivatives tested in the current study, NB15 was clearly the most effective inhibitor as determined in these assays. This compound maintained the *para*-hydroxyl orientation of G6, but had a minimized stilbenoid core. Based on the results obtained here, we conclude that having a minimized stilbenoid core on the *para*-hydroxyl structure provides the highest degree of Jak2 specific inhibition.

In summary, we have identified important structural features of the Jak2 small molecule inhibitor G6. We found that the *para*-hydroxyl structure with a reduced stilbene core conferred strong Jak2 interactions in silico as well as greater Jak2 inhibitory potential in vitro and ex vivo as measured by reduced cell viability, reduced Jak2 kinase activity, reduced levels of phospho-STAT, increased cell cycle arrest and apoptosis and reduced Jak2 clonogenic growth potential. As such, these results may be useful in the future development of stilbene-derived Jak2 inhibitors for the purpose of treating Jak2-mediated pathologies.

#### Acknowledgments

We thank Christopher Fuhrman for assistance with the molecular docking experiments. We thank Steve McClellan for assistance with flow cytometry. We also thank Anurima Majumder for significant intellectual contribution. This work was supported by National Institutes of Health Award R01-HL67277, a University of Florida Opportunity Fund Award, and a University of Florida/Moffitt Cancer Center Collaborative Initiative Award.

#### Supplementary data

Supplementary data associated with this article can be found, in the online version, at doi:10.1016/j.bmcl.2011.12.042.

## References and notes

1. Witthuhn, B. A.; Quelle, F. W.; Silvennoinen, O.; Yi, T.; Tang, B.; Miura, O.; Ihle, J. N. *Cell* **1993**, *74*, 227.
2. Argetsinger, L. S.; Campbell, G. S.; Yang, X. N.; Witthuhn, B. A.; Silvennoinen, O.; Ihle, J. N.; Carters, C. *Cell* **1993**, *74*, 237.
3. Sattler, M.; Durstin, M. A.; Frank, D. A.; Okuda, K.; Kaushansky, K.; Salgia, R.; Griffin, J. D. *Exp. Hematol.* **1995**, *23*, 1040.
4. Parganas, E.; Wang, D.; Stravopodis, D.; Topham, D. J.; Marine, J. C.; Teglund, S.; Vanin, E. F.; Bodner, S.; Colamonici, O. R.; van Deursen, J. M.; Grosveld, G.; Ihle, J. N. *Cell* **1998**, *93*, 385.
5. Zhao, L.; Ma, Y.; Seemann, J.; Huang, L. J. *Biochem. J.* **2010**, *426*, 91.
6. Gnanasambandan, K.; Magis, A.; Sayeski, P. P. *Biochemistry* **2010**, *49*, 9972.
7. James, C.; Ugo, V.; Le Couedic, J. P.; Staerk, J.; Delhommeau, F.; Lacout, C.; Garcon, L.; Raslova, H.; Berger, R.; Bennaceur-Griscelli, A.; Villeval, J. L.; Constantinescu, S. N.; Casadevall, N.; Vainchenker, W. *Nature* **2005**, *434*, 1144.
8. Kralovics, R.; Passamonti, F.; Buser, A. S.; Teo, S. S.; Tiedt, R.; Passweg, J. R.; Tichelli, A.; Cazzola, M.; Skoda, R. C. N. *Engl. J. Med.* **2005**, *352*, 1779.
9. Levine, R. L.; Wadleigh, M.; Coombs, J.; Ebert, B. L.; Wernig, G.; Huntly, B. J.; Boggon, T. J.; Wlodarska, I.; Clark, J. J.; Moore, S.; Adelsperger, J.; Koo, S.; Lee, J. C.; Gabriel, S.; Mercher, T.; D'Andrea, A.; Frohling, S.; Dohner, K.; Marynen, P.; Vandenberghe, P.; Mesa, R. A.; Tefferi, A.; Griffin, J. D.; Eck, M. J.; Sellers, W. R.; Meyerson, M.; Golub, T. R.; Lee, S. J.; Gilliland, D. G. *Cancer Cell* **2005**, *7*, 387.
10. Zhao, R.; Xing, S.; Li, Z.; Fu, X.; Li, Q.; Krantz, S. B.; Zhao, Z. J. *J. Biol. Chem.* **2005**, *280*, 22788.
11. Baxter, E. J.; Scott, L. M.; Campbell, P. J.; East, C.; Fourouclas, N.; Swanton, S.; Vassiliou, G. S.; Bench, A. J.; Boyd, E. M.; Curtin, N.; Scott, M. A.; Erber, W. N.; Green, A. R. *Lancet* **2005**, *365*, 1054.
12. Bumm, T. G.; Elsea, C.; Corbin, A. S.; Loriaux, M.; Sherbenou, D.; Wood, L.; Deininger, J.; Silver, R. T.; Druker, B. J.; Deininger, M. W. *Cancer Res.* **2006**, *66*, 11156.
13. Xing, S.; Wanting, T. H.; Zhao, W.; Ma, J.; Wang, S.; Xu, X.; Li, Q.; Fu, X.; Xu, M.; Zhao, Z. J. *Blood* **2008**, *111*, 5109.
14. Kiss, R.; Sayeski, P. P.; Keseru, G. M. *Expert Opin. Ther. Pat.* **2010**, *20*, 471.
15. Kiss, R.; Polgar, T.; Kirabo, A.; Sayyah, J.; Figueroa, N. C.; List, A. F.; Sokol, L.; Zuckerman, K. S.; Gali, M.; Bisht, K. S.; Sayeski, P. P.; Keseru, G. M. *Bioorg. Med. Chem. Lett.* **2009**, *19*, 3598.
16. Kirabo, A.; Embury, J.; Kiss, R.; Polgar, T.; Gali, M.; Majumder, A.; Bisht, K. S.; Cogle, C. R.; Keseru, G. M.; Sayeski, P. P. *J. Biol. Chem.* **2011**, *286*, 4280.
17. Majumder, A.; Govindasamy, L.; Magis, A.; Kiss, R.; Polgar, T.; Baskin, R.; Allan, R. W.; Agbandje-McKenna, M.; Reuther, G. W.; Keseru, G. M.; Bisht, K. S.; Sayeski, P. P. *J. Biol. Chem.* **2010**, *285*, 31399.
18. Lucet, I. S.; Fantino, E.; Styles, M.; Bamert, R.; Patel, O.; Broughton, S. E.; Walter, M.; Burns, C. J.; Treutlein, H.; Wilks, A. F.; Rossjohn, J. *Blood* **2006**, *107*, 176.
19. Huey, R.; Morris, G. M.; Olson, A. J.; Goodsell, D. S. *J. Comput. Chem.* **2007**, *28*, 1145.
20. Morris, G. M.; Goodsell, D. S.; Halliday, R. S.; Huey, R.; Hart, W. E.; Bewley, R. K.; Olson, A. J. *J. Comput. Chem.* **1998**, *19*, 1639.
21. Nosaka, T.; Kawashima, T.; Misawa, K.; Ikuta, K.; Mui, A. L.; Kitamura, T. *EMBO J.* **1999**, *18*, 4754.
22. Gesbert, F.; Griffin, J. D. *Blood* **2000**, *96*, 2269.
23. King, R. W.; Jackson, P. K.; Kirschner, M. W. *Cell* **1994**, *79*, 563.
24. Knoblich, J. A.; Lehner, C. F. *EMBO J.* **1993**, *12*, 65.
25. Gross, A.; Yin, X. M.; Wang, K.; Wei, M. C.; Jockel, J.; Milliman, C.; Erdjument-Bromage, H.; Tempst, P.; Korsmeyer, S. J. *J. Biol. Chem.* **1999**, *274*, 1156.
26. Gomez-Bougie, P.; Oliver, L.; Le Gouill, S.; Bataille, R.; Amiot, M. *Oncogene* **2005**, *24*, 8076.
27. Scoltock, A. B.; Cidlowski, J. A. *Exp. Cell Res.* **2004**, *297*, 212.
28. Kirabo, A.; Park, S. O.; Majumder, A.; Gali, M.; Reinhard, M. K.; Wamsley, H. L.; Zhao, Z. J.; Cogle, C. R.; Bisht, K. S.; Keseru, G. M.; Sayeski, P. P. *Neoplasia* **2011**, *13*, 1058.
29. Kelkel, M.; Jacob, C.; Dicato, M.; Diederich, M. *Molecules* **2010**, *15*, 7035.